

# Supplemental material

## Stability of ablation flows in inertial confinement fusion: non-modal effects

G. Varillon,<sup>1,2</sup> J.-M. Clarisse,<sup>1</sup> and A. Couairon<sup>2</sup>

<sup>1</sup>CEA, DAM, DIF, F-91297 ArpaJon, France

<sup>2</sup>CPHT, CNRS, Ecole Polytechnique, Institut Polytechnique de Paris, Route de Saclay, 91128 Palaiseau, France\*

(Dated: July 7, 2020)

### I. BASIC NOTIONS OF NON-MODAL ANALYSIS

For a time-dependent evolution operator as in Eq. 3, the growth of the state variable  $\widehat{\mathbf{U}}$  can be assessed at any given time  $t_*$  from the instantaneous growth rate of some chosen norm of  $\widehat{\mathbf{U}}$ , namely [1]

$$\sigma(t_*) \equiv \left( \frac{1}{\|\widehat{\mathbf{U}}\|^2} \frac{d\|\widehat{\mathbf{U}}\|^2}{dt} \right) \Big|_{t_*} = 2 \operatorname{Re} \left( \frac{\langle \widehat{\mathbf{U}}, \mathcal{A} \widehat{\mathbf{U}} \rangle}{\langle \widehat{\mathbf{U}}, \widehat{\mathbf{U}} \rangle} \right) \Big|_{t_*},$$

where  $\langle \cdot, \cdot \rangle$  denotes the scalar product associated to this norm and  $\|\widehat{\mathbf{U}}\|^2 = \langle \widehat{\mathbf{U}}, \widehat{\mathbf{U}} \rangle$ . The ratio

$$\frac{\langle \widehat{\mathbf{U}}, \mathcal{A} \widehat{\mathbf{U}} \rangle}{\langle \widehat{\mathbf{U}}, \widehat{\mathbf{U}} \rangle} \Big|_{t_*},$$

is known as the *numerical range* of the operator  $\mathcal{A}|_{t_*}$  and defines a convex region of the complex plane that contains the spectrum of  $\mathcal{A}|_{t_*}$ . In the general case of a non-normal operator, the numerical range is larger than the convex hull of the spectrum. In the case of a normal operator, the two regions coincide [2]. In particular, this numerical range may protrude into the unstable half-plane ( $\operatorname{Re} > 0$ ) even though the spectrum of  $\mathcal{A}|_{t_*}$  may be confined to the stable half-plane ( $\operatorname{Re} < 0$ ): cf. Fig. 1(c). In such a case *non-modal growth* occurs, i.e. an initial amplification – *transient growth* – of  $\widehat{\mathbf{U}}$  may be observed, although all eigenvalues are stable according to modal stability analysis. The potential for such a transient growth is measured by means of the maximum of the instantaneous growth rate  $\sigma(t_*)$  over all non-zero possible states, or *numerical abscissa* of  $\mathcal{A}|_{t_*}$ , say  $\sigma_* \equiv \max_{\widehat{\mathbf{U}}} \sigma(t_*)$ . This numerical abscissa is given by the largest eigenvalue of the normal operator  $(\mathcal{A} + \mathcal{A}^\dagger)|_{t_*}$  and is achieved when  $\widehat{\mathbf{U}}$  is the principal eigenfunction of this operator (cf. Ref. 1), thus defining the *optimal-growth initial condition* at time  $t_*$ , say  $\widehat{\mathbf{U}}_*^{\text{opt}}$ . The situation of non-normal growth described above corresponds to the case  $\max \operatorname{Re}(\Lambda) < 0 < \sigma_*$ , where  $\Lambda$  denotes the eigenvalues of  $\mathcal{A}|_{t_*}$ . However non-modal effects are not restricted to this specific configuration. Indeed, when  $0 < \max \operatorname{Re}(\Lambda) < \sigma_*$  [Fig. 1(b)], the system is unstable at all time horizons but may display a transient growth that is faster than the exponential growth of the least stable eigenfunction. For  $\max \operatorname{Re}(\Lambda) < \sigma_* \leq 0$  [Fig. 1(a)], the system is stable, here again at all time horizons, but with an eventual transient decay that is slower than the exponential decay of the least stable eigenfunction.

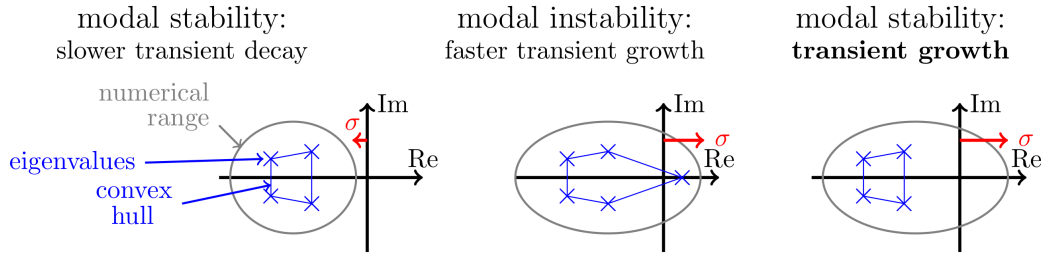


FIG. 1: Schematic layouts in the complex plane of eigenvalues and numerical ranges corresponding to: (a) modal stability with slower non-modal transient decay, (b) modal instability with faster non-modal transient growth, and (c) modal stability with non-modal transient growth.

\*gregoire.varillon@polytechnique.edu

## II. CONNECTION WITH A CAPSULE IMPLOSION SIMULATION

The solution  $(\mathcal{B}_\phi, \mathcal{B}_p) = (0.8, 0.31)$  of Eqs. 1, 2 has been chosen among a large set of self-similar ablation waves [cf. 3] on the basis of its hydrodynamic characteristic numbers which are typical of the early stage of a capsule implosion flow – the so-called *shock transit stage* during which the leading shock front of the ablation wave has not yet reached the ablator inner surface. During this stage, neither the radiative heat flux at the capsule external surface, nor the pressure exerted by the hohlraum filling gas, nor the capsule ablator opacity comply with the constraints required for self-similarity. In addition, the effects on the ablation flow of the spectral content of hohlraum x-rays cannot be rendered by the approximation of radiative heat conduction that leads to Eq. 1. The present modeling of radiative ablation compares however favorably with any of the models previously used for investigating hydrodynamic stability of ablation flows and designing experiments. In this respect, results obtained with the chosen self-similar ablation wave may be equally used in connection with capsule ablation simulations.

Considering a particular ICF capsule design (here that given in Ref. 4, Fig. 1) and its implosion simulation with an ICF hydrocode (code FCI2, cf. Ref. 5), time and length scales may be defined respectively from the duration of the ablation flow regime within the period of the shock transit stage, and the distance travelled by the leading shock front during this period. The starting time of this ablation regime is established as being one of the earliest times for which, in the simulation, an ablation wave structure with a non-vanishing extent of its shock-compressed region is clearly identified within the ablator, presently  $\bar{t}_0 = 2.8$  ns. This starting time is associated to the reference time of the self-similar ablation wave which may be set arbitrarily to be  $t_0 = 1$ . The final time of the ablation regime, in the simulation, is taken to be the time of the shock-front breakout at the ablator inner surface, here  $\bar{t}_1 = 12.9$  ns. Over the flow period thus defined, a linear perturbation initiated at the ablation front may propagate as a forward acoustic wave towards the shock front then back to the ablation front as an advected entropy wave [6], the whole being repeated a limited number of times. This finite sequence of propagation-then-advection of perturbations between the ablation and shock fronts is a key mechanism of perturbation dynamics during the shock-transit stage: e.g. see Refs. [7, 8]. Seeking to reproduce the same wave sequence in the present self-similar flow is therefore desirable, and presently sets a lower bound on the maximum time horizon for this flow, here  $t_1 = 8$ . The correspondence of flow durations and shock travel distances between the simulated flow and the self-similar solution defines then time and length scales for the latter, in effect  $t_\star = 1.44$  ns and  $l_\star = 19.04$   $\mu\text{m}$ .

- 
- [1] P. J. Schmid and D. S. Henningson, *Stability and transition in shear flows* (Springer, 2001).
  - [2] R. A. Horn and C. R. Johnson, *Matrix Analysis* (Cambridge University Press, 1990).
  - [3] J.-M. Clarisse et al., *J. Fluid Mech.* **848**, 219 (2018).
  - [4] Y. Saillard, *C. R. Acad. Sci. Paris, Series IV* **1**, 705 (2000).
  - [5] E. Buresi et al., *Laser Part. Beams* **4**, 531 (1986).
  - [6] G. Varillon et al., *Phys. Rev. E* **101**, 043215 (2020).
  - [7] V. N. Goncharov et al., *Phys. Plasmas* **7**, 2062 (2000).
  - [8] Y. Aglitskiy et al., *Phil. Trans. R. Soc. A* **368**, 1739 (2010).